Chemical Science

EDGE ARTICLE

View Article Online
View Journal | View Issue

Cite this: *Chem. Sci.*, 2018, **9**, 7528

All publication charges for this article have been paid for by the Royal Society of Chemistry

Reversible π-system switching of thiophene-fused thiahexaphyrins by solvent and oxidation/reduction†

Tomohiro Higashino,*[a] Atsushi Kumagai,[a] Shigeyoshi Sakaki[b] and Hiroshi Imahori*[ac]

The concept of chemical topology has generated considerable interest among chemists and one of the state-of-the-art topics is Möbius topology in cyclic π-conjugated molecules. In this regard, expanded porphyrins have been extensively studied because of their facile topological interconversions and attractive optoelectronic properties. A typical example involves [28]hexaphyrins: they show topological conversion between planar Hückel and twisted Möbius topologies owing to their flexible structure. With this in mind, we designed a [28]hexaphyrin where one dimethine pyrrole unit was replaced with dithieno[3,4-*b*:3′,4′-*d*]thiophene (β-DTT), aiming at a reversible switching between macrocyclic and cross-conjugated π-systems by a change in molecular topologies. Considering that the β-DTT unit can offer both macrocyclic and cross-conjugated π-circuits, we envisioned that a combination of the topological interconversion of [28]hexaphyrin with the two π-circuits of the β-DTT unit would enable a reversible switching between macrocyclic and cross-conjugated π-circuits on Möbius and Hückel topologies, respectively, by a simple conformational change. Unexpectedly, the hexaphyrin revealed a unique, unprecedented π-system switching between a Möbius cross-conjugated π-system and a Hückel antiaromatic π-system, which was fully supported by both experimental and theoretical investigations. Meanwhile, the [28]hexaphyrin was also found to be redox interconvertible with the corresponding [26]hexaphyrin with a Hückel cross-conjugated π-system. These results demonstrate that the β-DTT unit is a new effective motif to realize π-system switching by changing molecular and π-system topologies. Importantly, external stimuli, *i.e.*, solvent, as well as oxidation/reduction can be used to trigger the topological changes in expanded porphyrins with the help of the β-DTT unit.

Received 4th June 2018
Accepted 7th August 2018

DOI: 10.1039/c8sc02448k

rsc.li/chemical-science

Introduction

The concept of chemical topology, which was defined by Frisch and Wasserman in 1961,[1] has evoked considerable interest among chemists. To date, various molecular knots, links,[2] and polymers[3] have been synthesized as topological molecules. Among the chemical topologies, Möbius topology is one of the important topics in aromaticity, which is essential for understanding the energetic stability of cyclic π-conjugated molecules. In general, the Hückel rule can be applied to predict whether a cyclic molecule is aromatic or antiaromatic. If the cyclic molecule has $[4n+2]\pi$ or $[4n]\pi$ electrons, it should be aromatic or antiaromatic, respectively. On the other hand, for the singly half-twisted cyclic molecule as a Möbius strip, Heilbronner predicted that the $[4n+2]\pi$ and $[4n]\pi$ electron rules should be reversed.[4] Namely, the cyclic molecules with $[4n]\pi$ and $[4n+2]\pi$ electrons on Möbius topology are aromatic and antiaromatic, respectively. Much attention has been devoted to this Möbius aromaticity; however, the synthesis of Möbius aromatic molecules has been a challenge because of the difficulty in balancing between their twisted structure and cyclic π-conjugation. Nevertheless, Herges and co-workers reported the synthesis of the first Möbius aromatic molecule in 2003.[5] After this seminal work, various porphyrinoids have been found to be Möbius aromatic[6,7] and antiaromatic[8] molecules.

Compared to typical porphyrins possessing four pyrrole units, expanded porphyrins, which consist of more than four pyrrole units, exhibit a flexible structure. They have attracted significant attention because of their fascinating properties such as intense absorption in the near-infrared region, large two-photon absorption (TPA) cross section, and facile aromatic–antiaromatic switching upon two-electron oxidation/reduction or topological interconversions.[9,10] In particular, noteworthy are

[a]*Department of Molecular Engineering, Graduate School of Engineering, Kyoto University, Nishikyo-ku, Kyoto 615-8510, Japan. E-mail: t-higa@scl.kyoto-u.ac.jp; imahori@scl.kyoto-u.ac.jp*

[b]*Fukui Institute for Fundamental Chemistry, Kyoto University, Sakyo-ku, Kyoto 606-8103, Japan*

[c]*Institute for Integrated Cell-Material Sciences (WPI-iCeMS), Kyoto University, Sakyo-ku, Kyoto 606-8501, Japan*

† Electronic supplementary information (ESI) available: Synthesis, high-resolution mass spectra, NMR spectra, X-ray crystallographic details, absorption spectra, cyclic voltammograms, and DFT calculations. CCDC 1841655 and 1841656. For ESI and crystallographic data in CIF or other electronic format see DOI: 10.1039/c8sc02448k

their optical and photophysical properties that can be altered greatly by their topologies and π-systems.[11] In addition, topology and aromaticity switches based on expanded porphyrins have attracted much interest.[11d,e] Thus, expanded porphyrins could be ideal platforms for exploring novel functions as well as addressing fundamental aspects of chemical topology by rational molecular design. To date, protonation has been one of the effective means to achieve topological interconversions,[7b,d,i,12] while solvent-dependent topological switching is still rare.[7a,13]

Recently, we synthesized octaphyrins where two dimethine pyrrole units were replaced with two dithieno[3,4-*b*:3′,4′-*d*] thiophene (β-DTT) units. We found that the β-DTT unit could yield two types of π-circuits depending on the oxidation state of the sulfur atom.[14] One is a macrocyclic π-circuit with incorporation of the lone pair of the central sulfur atom, and the other is a cross-conjugated π-circuit without incorporation of the lone pair (Fig. 1a). As a result, octaphyrin **1** revealed a macrocyclic 36π-electron circuit, whereas octaphyrin **2** possessed a cross-conjugated π-circuit (Fig. 1b). Namely, the optical and electrochemical properties of the octaphyrins can be altered by the corresponding change from the macrocyclic to the cross-conjugated π-system. This transformation is basically similar to that of N-confused porphyrins, which exhibit reversible π-system switching between 18π aromatic and cross-conjugated systems by NH tautomerism (Fig. 1c).[15] However, it is impossible to achieve reversible π-switching between **1** and **2** because the transformation of **1** to **2** is based on chemical oxidation on the sulfur atom. We also examined the redox interconversions of **1** between 36π and 34π-electrons, or 36π and 38π-electrons, but the attempts failed probably due to the presence of the two β-DTT units, which is consistent with no examples of core-modified expanded porphyrins exhibiting reversible redox interconversions.[16]

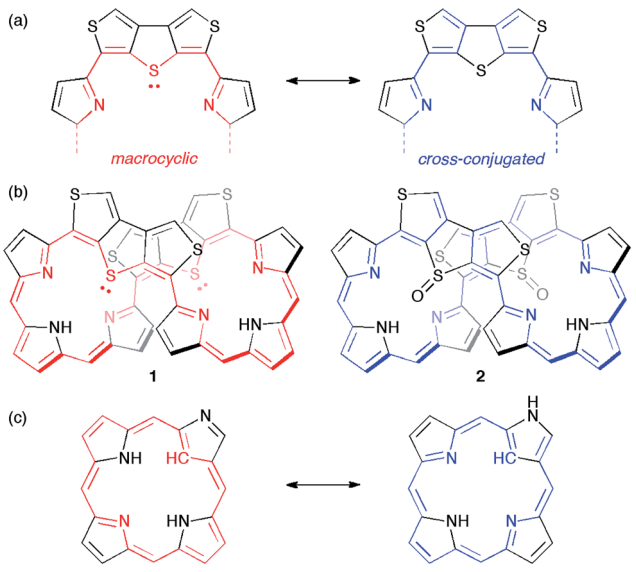

Fig. 1 (a) Two types of π-circuits of the β-DTT unit. (b) Representation of π-circuits of the octaphyrins with the β-DTT unit. (c) Two NH tautomers of the N-confused porphyrin (NCP).

Herein, to realize the reversible switching between macrocyclic and cross-conjugated π-systems on expanded porphyrins, we designed a [28]hexaphyrin where one dimethine pyrrole unit was replaced with one β-DTT unit. Typical [28]hexaphyrins are known to exhibit topological conversion between planar Hückel and twisted Möbius topologies because of their flexible structure (Fig. 2a).[6b] The Hückel and Möbius topologies lead to the antiaromatic and aromatic character, respectively. In general, aromatic systems are energetically favorable compared to antiaromatic ones. Indeed, the typical [28]hexaphyrin shows a distinct aromatic character in solution. On the basis of the two topologies of [28]hexaphyrin and the two types of π-circuits of the β-DTT unit, we envisioned the following four π-system topologies (Fig. 2b): (1) Möbius macrocyclic (**28MM**), (2) Möbius cross-conjugated (**28MC**), (3) Hückel macrocyclic (**28HM**), and (4) Hückel cross-conjugated (**28HC**) π-systems. On the Möbius topology, a macrocyclic 28π-circuit gains Möbius aromatic stabilization, but a cross-conjugated π-circuit weakens the aromatic stabilization. Accordingly, the Möbius topology would prefer the macrocyclic 28π-electron circuit. In contrast, a macrocyclic π-circuit on the Hückel topology is unfavorable because of the Hückel antiaromaticity, whereas a cross-conjugated π-circuit decreases the antiaromatic destabilization. Namely, the cross-conjugated π-circuit would be suitable on the Hückel topology. Overall, we predicted reversible switching between the macrocyclic π-circuit on the Möbius topology and the cross-conjugated π-circuit on the Hückel topology by a simple conformational change. Meanwhile, hexaphyrins can exhibit reversible redox interconversions between 28π and 26π-electron systems (Fig. 2a). Typical [26]hexaphyrins take a planar Hückel topology, but [26]hexaphyrins with the Möbius topology have not been reported because of the plausible instability of their Möbius antiaromaticity.[6c,f] Although the Möbius topology is unfavorable for [26]hexaphyrins, we can also make a list of the four π-system topologies, as proposed for [28]hexaphyrin (Fig. 2b). Taking into account that typical [26]hexaphyrins prefer the Hückel topology, we anticipated that a [26]hexaphyrin with the β-DTT unit would possess a macrocyclic π-system on the Hückel topology (**26HM**), and if possible, cross-conjugated π-system on the Möbius topology (**26MC**). Thus, a combination of the redox interconversions between [28]hexaphyrin and [26]hexaphyrin with the change in molecular topologies would accomplish the three-component reversible π-system switching between (1) 28π Möbius macrocyclic (**28MM**), (2) 28π Hückel cross-conjugated (**28HC**), and (3) 26π Hückel macrocyclic (**26HM**) π-systems. In this work, we describe the synthesis and characterization of hexaphyrins with the β-DTT unit and unexpected, unprecedented π-system switching with full support of theoretical calculations.

Results and discussion

Synthesis and characterization

Synthetic schemes of the hexaphyrins with the β-DTT unit are shown in Scheme 1. The acid-catalyzed condensation of bis(pyrrolyl)dithienothiophene **3**[14] and tripyrrane dicarbinol **4**,[17] followed by oxidation with 2,3-dichloro-5,6-dicyanobenzoquinone

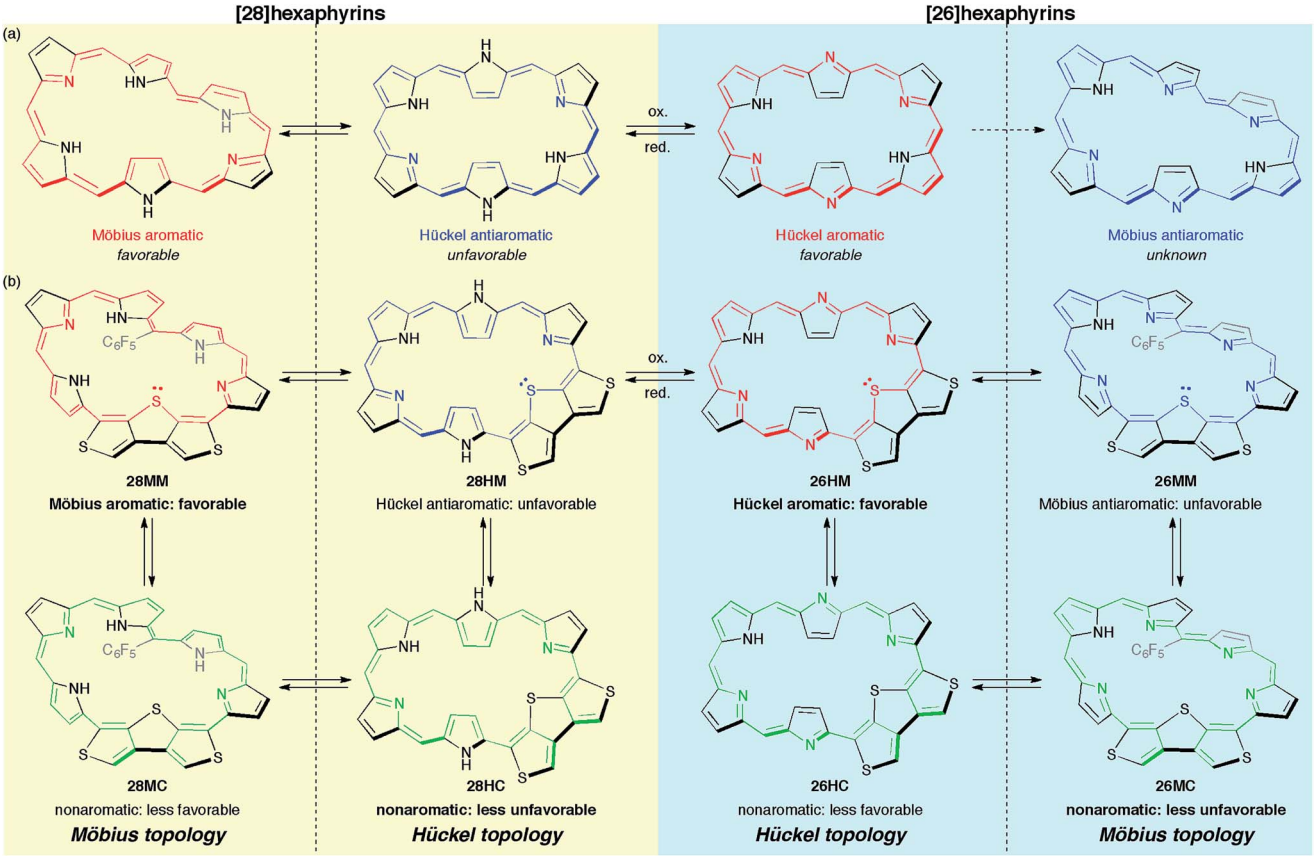

Fig. 2 (a) Molecular topologies of [28]hexaphyrin and [26]hexaphyrin. (b) Possible π-system topologies of hexaphyrins with the β-DTT unit on Hückel and Möbius topologies.

(DDQ), afforded [28]hexaphyrin **5** in 6.9% yield. The high-resolution mass spectrum (HRMS) of **5** exhibits an ion peak at m/z = 1234.0210 (calcd for $C_{56}H_{16}N_5F_{20}S_3$, $[M + H]^+$: 1234.0243), which matches with its 28π electronic state (Fig. S1†). Then, we attempted the redox interconversion and found that [28]hexaphyrin **5** and [26]hexaphyrin **6** were quantitatively interconvertible through oxidation with MnO_2 and reduction with $NaBH_4$. To the best of our knowledge, **6** is the first example of thia[26]hexaphyrin.[18] It is noteworthy that further reduction of **5** and oxidation of **6** resulted in decomposition without formation of the corresponding [30]hexaphyrin and [24]hexaphyrin.

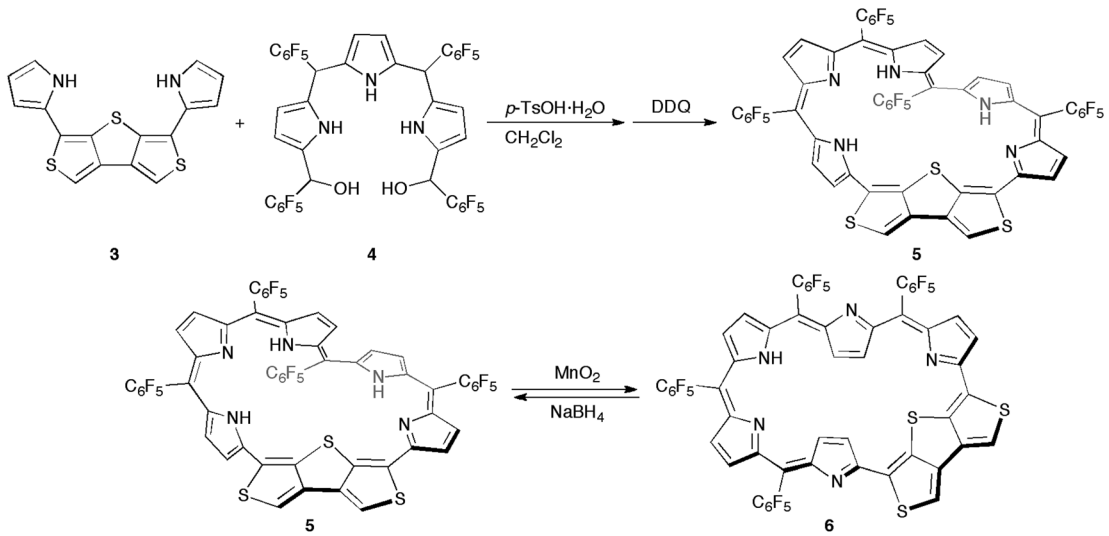

Scheme 1 Synthesis of thiophene-fused thiahexaphyrins **5** and **6**.

Fortunately, we obtained single crystals suitable for X-ray diffraction analysis by vapor diffusion of *n*-hexane into a CH_2Cl_2 solution of **5**. The structure of **5** was revealed to be a twisted Möbius structure (Fig. 3a and S5†).‡ The structure of **5** also showed bond length alternation to a certain extent. Although this suggests the antiaromatic or nonaromatic character of **5**, it is difficult to distinguish between the antiaromatic macrocyclic π-circuit and nonaromatic cross-conjugated π-circuit from the X-ray crystal structure of **5**. Because of the rigidity of the β-DTT unit, the pyrrole A neighboring the β-DTT unit is significantly tilted. Consequently, the torsion angle at C(5)–C(6) is the largest value (66°). Although the largest torsion angle in the conjugation circuit of **5** is larger than those of typical Möbius aromatic [28]hexaphyrins (26–49°),[6] it is virtually identical to that of a [28]hexaphyrin monophosphorus complex (65°).[8b] The ^{1}H NMR spectra of **5** were measured in various solvents. The ^{1}H NMR spectrum in $CDCl_3$ displays the signals from β-protons at δ = 6.94–6.24 ppm, two signals from thiophene protons at δ = 7.67 and 7.62 ppm, and three signals from NH protons at δ = 13.09, 12.25, and 9.97 ppm (Fig. 4a). Contrary to our expectation from the crystal structure, the ^{1}H NMR spectrum implies the nonaromatic character of **5** because those of nonaromatic acyclic π-conjugated oligopyrromethenes show the characteristic signals of pyrrolic β-protons in the range of 6.0–6.7 ppm.[9c,19] On the other hand, the [28]hexaphyrin monophosphorus complex exhibits a moderate 28π Möbius aromatic character even with a large torsion angle.[8b] Namely, the large torsion angle (66°) of **5** would not interrupt the macrocyclic π-circuit. Therefore, the nonaromatic character of **5** indicates that

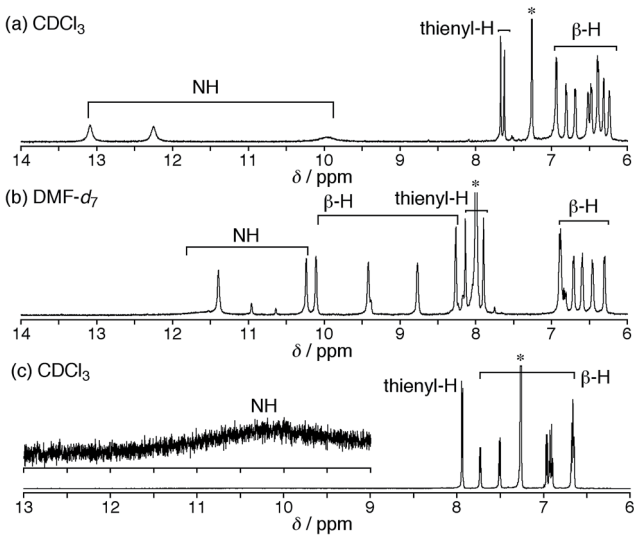

Fig. 4 ^{1}H NMR spectra of **5** in (a) $CDCl_3$ at 50 °C and (b) DMF-d_7 at 25 °C, and (c) **6** in $CDCl_3$ at 25 °C.

the cross-conjugated π-network arising from the β-DTT unit is dominant despite its Möbius structure. Remarkably, we found a dramatic solvent effect on the ^{1}H NMR spectra of **5**. In DMF-d_7, the spectrum displays four significantly deshielded signals from β-protons at δ = 10.14, 9.45, 8.80, and 8.30 ppm (Fig. 4b). The downfield shifts of β-protons imply a weak diatropic ring current effect originating from the weak 28π Möbius aromaticity with retention of the Möbius structure, or a weak

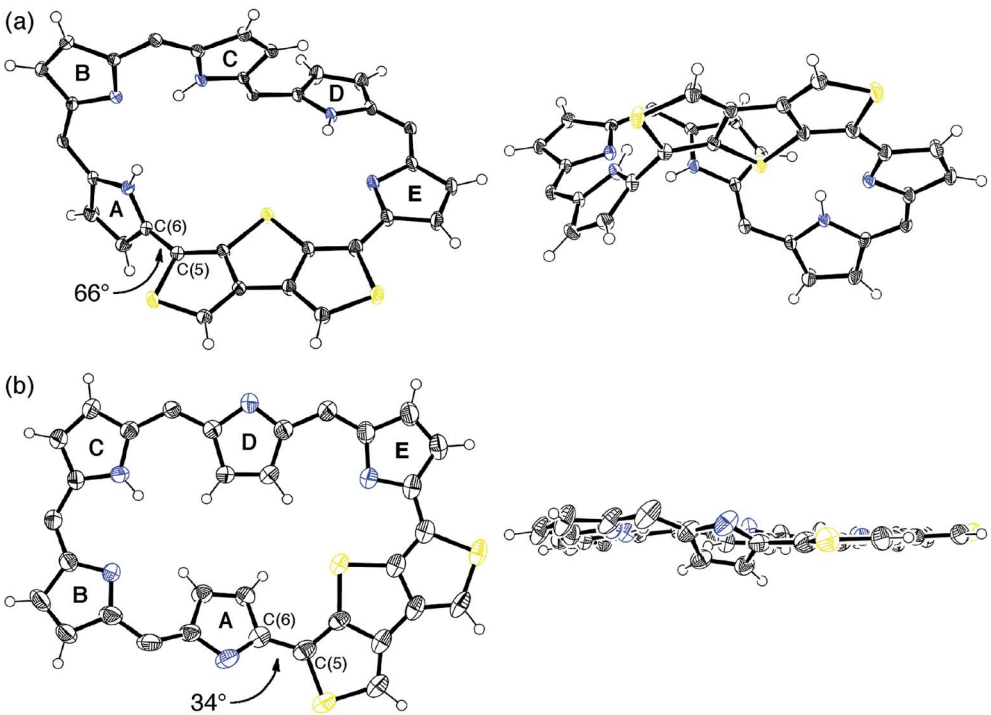

Fig. 3 X-Ray crystal structures of (a) **5** and (b) **6**: top view (left) and side view (right). For **6**, one of the two independent molecules in the unsymmetric unit cell is shown. Thermal ellipsoids represent 50% probability. *meso*-Aryl substituents, solvent molecules, and minor disorder components are omitted for clarity. The torsion angles at the most distorted points are indicated.

paratropic ring current effect originating from the weak 28π Hückel antiaromaticity on the different structures with Hückel topology.[9c] This means that the π-system of **5** can be switched between cross-conjugated and macrocyclic 28π-electron systems by solvent. In addition, the spectrum in acetone-d_6 at 25 °C shows two sets of peaks, the major one similar to those in DMF-d_7, and the minor one similar to those in $CDCl_3$ (Fig. S3†). The intensities of the minor peaks are increased at 50 °C, suggesting the equilibrium between two conformations. Therefore, [28]hexaphyrin **5** should adopt two conformations in solution. Namely, **5** takes a Möbius conformation as the crystal structure (obtained from a CH_2Cl_2 solution) with the cross-conjugated π-system in $CDCl_3$, whereas it takes a different conformation with a macrocyclic 28π-system in DMF-d_7. Unfortunately, we could not obtain single crystals from a solution in polar solvents (*i.e.*, DMF and acetone) to reveal the conformation despite extensive trials. Finally, by analyzing the results of density functional theory (DFT) calculations and simulated ^{1}H chemical shifts judiciously, we assigned the conformation in DMF-d_7 to a planar conformation exhibiting a 28π Hückel antiaromatic character (*vide infra*). Consequently, unexpectedly, the ^{1}H NMR spectra displayed the switching between cross-conjugated and macrocyclic π-circuits on Möbius and Hückel topologies, respectively, both of which were anticipated to be unfavorable energetically. It should be emphasized that we confirmed the reversibility by repeated measurements in both nonpolar and polar solvents.

Meanwhile, the structure of **6** was revealed to be a planar rectangular structure on the basis of X-ray diffraction analysis (Fig. 3b and S6†).‡ Basically, the bond length alternation also suggests the nonaromatic or antiaromatic character of **6**. Taking into account that a macrocyclic π-circuit on planar [26]hexaphyrin provides a 26π aromatic character, the bond alternation of **6** implies a nonaromatic cross-conjugated π-circuit. Although pyrrole A is tilted by 33° with respect to the mean-plane (core 36 atoms), the mean-plane deviation is rather small (*ca.* 0.20 Å), which can be ascribed to the rigid β-DTT unit. In the packing structure, the β-DTT unit and pyrrole E form one-dimensional π–π stacking motifs and the separation distance between the two planes is approximately 3.5 Å (Fig. S7†). The ^{1}H NMR spectrum of **6** in $CDCl_3$ displays ten signals of β-protons at δ = 7.73–6.67 ppm, two signals of thiophene protons at δ = 7.95 and 7.93 ppm, and one broad signal of NH proton at 10.11 ppm (Fig. 4c). This spectrum indicates the almost nonaromatic character of **6**, which is similar to those of cross-conjugated quinonoidal hexaphyrins.[20] Thus, the dominant π-circuit of **6** is a cross-conjugated π-network derived from the β-DTT unit, which is also contrary to our initial intuitive expectation. Compared to **5**, **6** displays a minor solvent effect on the ^{1}H NMR spectra, which suggests no significant conformational change in solution (Fig. S4†). Therefore, hexaphyrins with the β-DTT unit achieved three-component reversible π-system switching between 28π Möbius cross-conjugated, 28π Hückel macrocyclic, and 26π Hückel cross-conjugated π-systems by solvent-dependent topological or redox interconversions.

Optical and electrochemical properties

The UV/vis/NIR absorption spectra of **5** and **6** were measured in various solvents (Fig. 5). The spectrum of **5** in CH_2Cl_2 has a weak Soret-like band and weak and broad Q-like bands at 539 and 734 nm, respectively. The spectrum of **6** in CH_2Cl_2 also displays a weak Soret-like band at 487 nm and a broad Q-like band at 712 nm. These features are analogous to those of nonaromatic[20,21] and phlorin-type porphyrinoids,[22] which are consistent with the dominant nature of their cross-conjugated π-networks. In addition, as observed in the ^{1}H NMR spectra, the absorption spectra of **5** also exhibit the remarkable solvent effect (Fig. S8 and S9†). In polar solvents, the Q-like bands are red-shifted in the order of THF (837 nm) < methanol (965 nm) < acetone (1032 nm) < DMSO ≈ DMF (1044 nm). This trend suggests that hydrogen bonds of the NH protons with solvent molecules induce a π-system switching to the macrocyclic 28π-electron system. A moderate solvent effect in acetone can be rationalized by the equilibrium between the two conformations, which is seen in ^{1}H NMR spectroscopy. The spectrum of **5** in DMF displays an intense Soret-like band at 556 nm and Q-like bands at 940 and 1044 nm. Then, we also measured the steady-state fluorescence spectra of **5** and **6**. It should be noted that **5** exhibits no fluorescence in DMF, while **5** and **6** exhibit weak fluorescence at 955 and 930 nm in CH_2Cl_2, respectively (Fig. S10†). The weak fluorescence of **5** and **6** in CH_2Cl_2 is consistent with the cross-conjugated π-networks.[14] The optical properties of expanded porphyrins empirically enable us to judge whether they are aromatic or antiaromatic.[11c,23] Intriguingly, the intense Soret- and Q-like bands in DMF imply an aromatic character, whereas no fluorescence implies an antiaromatic character. Although the reason for these conflicting features is not clear at this stage, the replacement of one dimethine pyrrole with the β-DTT unit in [28]hexaphyrin plays an important role in the unusual optical properties. As described below, DFT calculations support the moderate 28π antiaromatic character of **5** in DMF and as far as we know, [28]hexaphyrin **5** is the sole exception among antiaromatic expanded porphyrins with both intense Soret- and Q-like bands, whereas antiaromatic porphyrinoids with only an intense Soret-band have been reported.[24]

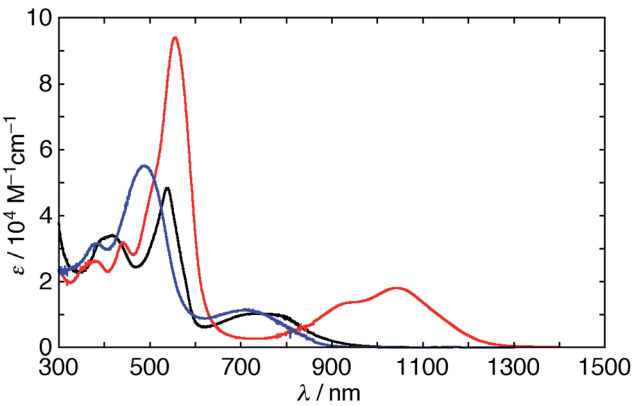

Fig. 5 UV/vis/NIR absorption spectra of **5** in CH_2Cl_2 (black) and DMF (red) and **6** in CH_2Cl_2 (blue).

The electrochemical properties of **5** and **6** were studied by using cyclic voltammetry (CV) and differential pulse voltammetry (DPV) in CH_2Cl_2 *versus* ferrocene/ferrocenium ions (Fc/Fc^+) with tetrabutylammonium hexafluorophosphate (Bu_4NPF_6) as an electrolyte (Fig. S11†). [28]Hexaphyrin **5** exhibits three irreversible reductions at −1.19, −1.41, and −1.83 V and two reversible oxidations at −0.03 and +0.28 V. These values are similar to those of a typical [28]hexaphyrin.[22e] On the other hand, [26]hexaphyrin **6** shows three reversible reductions at −0.13, −0.59 and −0.91 V, while no oxidation peak is observable. The more positive reduction potentials of **6** than those of the typical [26]hexaphyrin (−0.55 and −0.88 V)[20] can be rationalized by the cross-conjugated character.

DFT calculations

DFT calculations were carried out to shed light on the unique π-system switching of [28]hexaphyrin **5**. We performed optimization at the B3LYP/6-31G(d,p) level in the gas phase and obtained the optimized structure of **5a** using the crystal structure as the initial geometry (Fig. 6a). Assuming that **5** adopts different conformations in DMF, we explored metastable conformations by structural optimization using various initial geometries in which the tilt angles of pyrroles A and D were varied. Finally, we obtained three metastable conformations, planar Hückel conformations **5b** and **5c** (Fig. 6b and c) and Möbius conformation **5d** (Fig. 6d). The largest torsion angles in the conjugation circuit of **5b** (46°) and **5c** (44°) are smaller than that of **5a** (60°). On the other hand, the largest torsion angle of **5d** (63°) is slightly larger than that of **5a**. The relative total energies of **5b**, **5c**, and **5d** are calculated at the B3LYP/6-311G(d,p) level to be +18.4, +39.3, and +39.5 kJ mol^{-1}, respectively. The relative total energies calculated at CAM-B3LYP/6-311G(d,p) and M06-2X/6-311G(d,p) levels are consistent with those at B3LYP/6-311G(d,p) (Table S2†).[25] While conformations **5b** and **5d** possess one inverted pyrrole ring (pyrrole A), conformation **5c** possesses two inverted pyrrole rings (pyrroles A and D).

Then, we simulated ^{1}H chemical shifts on the three conformations **5a–d** using the gauge-including atomic orbital (GIAO) method at the B3LYP/6-311G(d,p) level (Fig. S12 and S13†). The ^{1}H chemical shift values were calculated with reference to $CHCl_3$ ($\delta = 7.26$ ppm). The simulated ^{1}H chemical shifts of the β-protons and two thiophene protons on **5a** are 7.27–6.51, and 7.88 and 7.83 ppm, respectively, which are in good agreement with the ^{1}H NMR spectrum of **5** in $CDCl_3$. For **5d**, the ^{1}H chemical shifts of the β-protons and two thiophene protons are 7.35–5.03, and 7.80 and 7.69 ppm, respectively. The upfield shifts of the β-protons on pyrrole A (6.32 and 5.03 ppm) are probably due to a local ring current effect induced by the pentafluorophenyl ring (Fig. S14†). Accordingly, these results predict the nonaromatic character of **5d**. In the case of **5b**, the simulated ^{1}H chemical shifts appear at 8.46–6.29 ppm for β-protons and 7.59 and 7.51 ppm for the two thiophene protons. It is noteworthy that β-protons on pyrrole A show clear downfield shifts (8.46 and 7.83 ppm), although the difference between the chemical shifts of the most shielded and deshielded β-protons is moderate ($\Delta\delta = 2.17$ ppm). These downfield shifts largely agree with the ^{1}H NMR spectrum of **5** in DMF-d_7 ($\Delta\delta = 3.80$ ppm). Since the β-protons on pyrrole A are located on the inside of the macrocycle, these chemical shifts suggest the 28π Hückel antiaromatic character on the planar conformation **5b**. Meanwhile, the simulated ^{1}H chemical shifts of β-protons for **5c** are 11.79–6.02 ppm. The β-protons on pyrroles A and D clearly exhibit a downfield shift (10.35 and 8.99 ppm for pyrrole A, 11.79 and 9.83 ppm for pyrrole D), which suggests the distinct 28π Hückel antiaromatic character. However, the large $\Delta\delta$

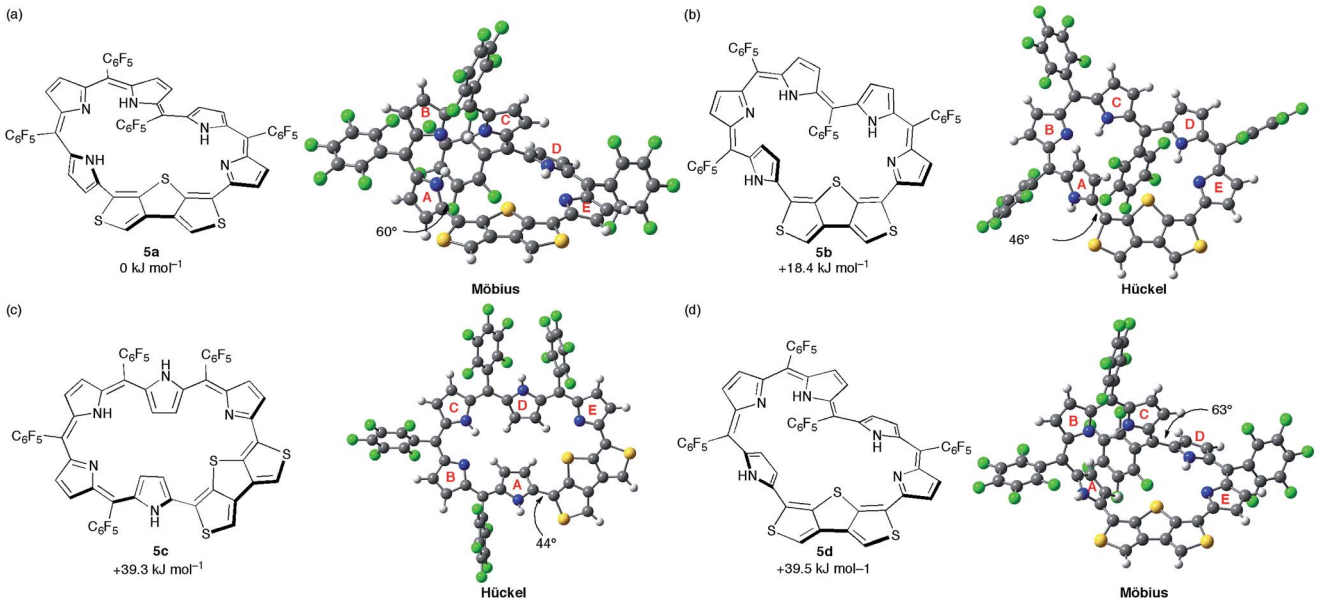

Fig. 6 The calculated conformations and relative total energies of [28]hexaphyrin: (a) **5a**, (b) **5b**, (c) **5c**, and (d) **5d**. The torsion angles at the most distorted points are indicated.

values of the β-protons (5.77 ppm) and two NH protons on pyrroles A and D (6.42 and 5.64 ppm) imply the mismatch with the ^{1}H NMR spectrum of **5** in DMF-d_7. Furthermore, we attempted to evaluate the antiaromatic character on **5b** and **5c**.[10b,26] Since the magnetic properties are sensitive to the aromaticity, we calculated the nucleus-independent chemical shift (NICS) values at the gravity centers of 36 core atoms (Table S3†).[27] The NICS value of **5b** is −0.14 ppm, which is less negative than those of **5a** (−0.57 ppm) and **5d** (−0.68 ppm). The NICS value of **5b** is almost zero due to the small $\Delta\delta$ value relative to those of typical antiaromatic [28]hexaphyrins ($\Delta\delta$ > 10 ppm).[6i,28] On the other hand, the small positive NICS value of **5c** (+2.48 ppm) implies the weak antiaromatic character, as suggested by the simulated ^{1}H chemical shifts. In addition, we also calculated the harmonic oscillator model of aromaticity (HOMA)[29] of **5a–d** to be −0.544, −0.651, −0.109, and −0.440, respectively. The negative HOMA values can be ascribed to their bond alternations, suggesting their almost nonaromatic character.

We also performed time-dependent DFT (TD-DFT) calculations to predict the absorption spectra at the B3LYP/6-311G(d,p) level on the optimized structures **5a–d** in the gas phase because the PCM solvation model exhibited negligible differences in excitation energies in various solvents (Fig. S15†). The calculated excitation energies and oscillator strengths for **5a** largely match with the absorption spectrum of **5** in CH_2Cl_2. If [28]hexaphyrin **5** has a macrocyclic π-circuit with zwitterionic character, the excitation energies should be increased in polar solvents. Thus, zwitterionic species of **5** should be excluded, although zwitterionic pyridinium-substituted [28]hexaphyrin was reported by Osuka and co-workers (Fig. 7).[30] The calculated excitation energies and oscillator strengths of **5b** and **5c** may reproduce intense Soret- and Q-like bands of **5** in DMF. The lowest excitation energies of **5b** (937 nm) and **5c** (1005 nm) are smaller than that of **5a** (829 nm), which is in good accordance with the red-shifted Q-like bands. On the other hand, the lowest excitation energy of **5d** (770 nm) is larger than that of **5a**, which is in contrast to the red-shifted Q-like bands of **5** in DMF. In addition, the Soret-like bands of **5b** and **5c** can be assigned to two excitations with large oscillator strengths (f > 0.4), which originate mainly from HOMO−1/LUMO and HOMO/LUMO+2 transitions. The high-energy transitions for the Soret-like bands of **5b** and **5c** are consistent with the fingerprints of antiaromaticity on the photophysical properties of expanded porphyrins.[24b] However, the distinct Q-like bands for the allowed HOMO/LUMO transitions are inconsistent with the fingerprints, as seen in the distinct Q-like band of **5** in DMF. Although the reason for the appearance of the distinct Q-like bands is not clear at this stage, the β-DTT unit in [28]hexaphyrin may play an important role in the unique photophysical properties. Combined with the relative total energies and the simulated ^{1}H chemical shifts, we can finally conclude that **5b** is the most probable conformation observed in DMF.

Nevertheless, it is rather difficult for **5** to take the conformation **5b** in solution considering the high relative total energy of **5b** (+18.4 kJ mol^{-1}). Given the stabilization by polar solvents, we conducted calculations for **5a** and **5b** using the PCM solvation model, but the relative total energy of **5b** was still large even

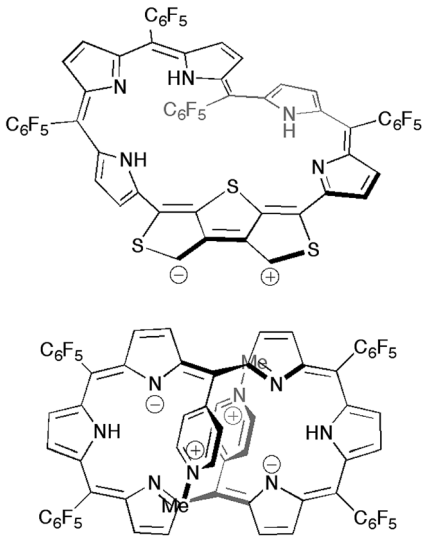

Fig. 7 Possible zwitterionic structures of [28]hexaphyrin **5** (top) in comparison to the methylpyridinium-substituted analogue (bottom).

in DMSO (*ca.* +14 kJ mol^{-1}). Surprisingly, the calculations of **5** in the presence of an explicit DMF molecule afford the negative relative total energy of **5b** (−6.2 kJ mol^{-1}) in comparison with **5a** (Fig. 8). The conformation **5b** is stabilized by a hydrogen bond of the NH proton of pyrrole A with the oxygen atom of the DMF molecule. The broad signal of the NH proton observed in the ^{1}H NMR spectrum is attributable to this hydrogen bond. Moreover, the relative total energy of **5b** in the presence of an acetone molecule is −0.4 kJ mol^{-1} (Fig. S16†). This small energy difference coincides with the equilibrium observed in the ^{1}H NMR spectra in acetone-d_6. The calculations using CAM-B3LYP and M06-2X as DFT functionals also afforded negative relative total energies of **5b** (Table S4†). Consequently, these calculations demonstrate that the hydrogen bond of the NH protons with polar solvent molecules induces the conformational change between Möbius conformation **5a** and planar conformation **5b**. The theoretical conclusion is contrary to our initial intuitive prediction that switching would occur between the Möbius aromatic π-system and Hückel cross-conjugated π-system. Indeed, the calculation supports the unique π-system switching of **5** between the Möbius cross-conjugated π-system and Hückel antiaromatic π-system on the basis of the change in molecular topologies, which is triggered by external stimuli (*i.e.*, solvent).

Meanwhile, we also performed DFT calculations for [26]hexaphyrin **6**. The ^{1}H chemical shifts of the β-protons and two thiophene protons are 7.94–6.29, and 8.36 and 8.28 ppm, respectively (Fig. S17†). The NICS value at the gravity center is −2.52 ppm. Thus, the NMR calculation supports the almost nonaromatic character of **6**. The calculated excitation energies and oscillator strengths reproduce the absorption spectrum of **6** (Fig. S18†). These results also verify the nonaromatic character, which is consistent with the cross-conjugated nature of **6**.

Finally, we sought to elucidate the origin of the dominant π-circuits of hexaphyrins **5** and **6**. To gain insight into the structural parameters, we calculated the bond lengths and Wiberg

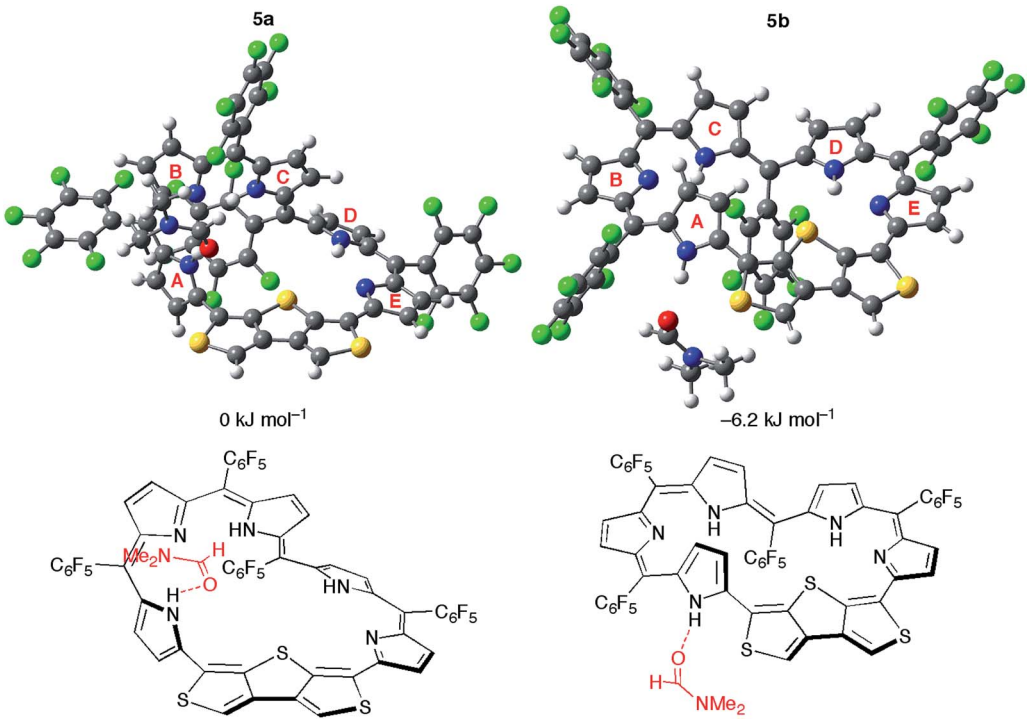

Fig. 8 The optimized structures and relative total energies of [28]hexaphyrin conformations **5a** and **5b** in the presence of one DMF molecule.

bond indices based on NAO (natural atomic orbital) on the β-DTT unit, but these values turned out to be almost the same (Table S5†). Thus, it is impossible to predict the dominant π-circuits from the structural parameters and bond orders on the β-DTT unit.[31] Then, we conducted DFT calculations of **3** as a model of the β-DTT unit (Fig. S19†). The HOMO of **3** has an orbital distribution on the central sulfur atom, which indicates the involvement of the p_z orbital of the sulfur atom (Fig. 9). In contrast, the HOMO−1 has no orbital distribution on the central sulfur atom, indicating no contribution of the p_z orbital. Additionally, the orbital phases on the two pyrrole rings are identical for the HOMO, or opposite for the HOMO−1. Notably,

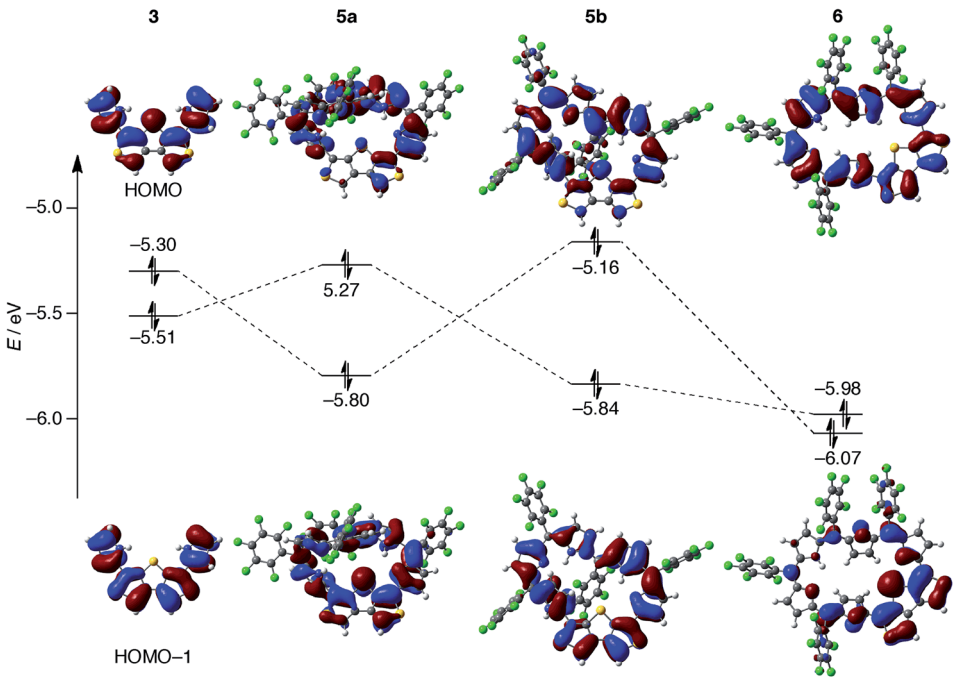

Fig. 9 Selected Kohn–Sham orbitals for **3**, **5a**, **5b**, and **6** that were calculated at the B3LYP/6-311G(d,p) level.

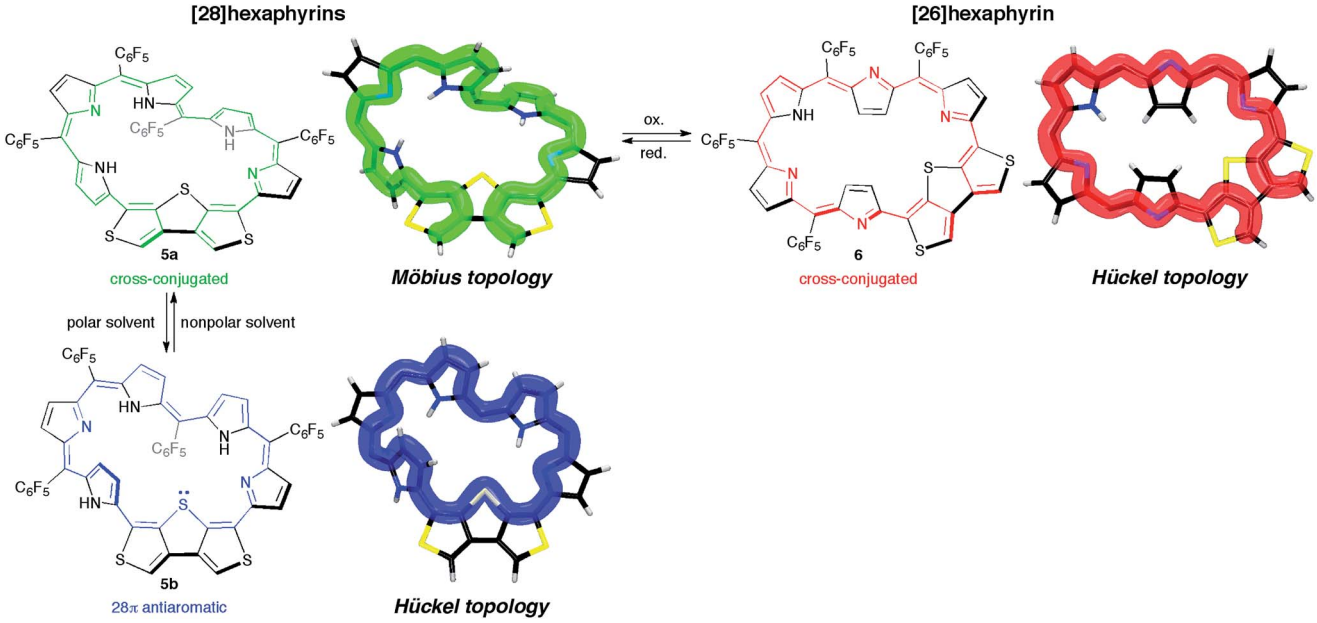

Fig. 10 Schematic representation of reversible π-system switching between hexaphyrins **5a**, **5b**, and **6**. *meso*-Aryl substituents are omitted for clarity.

the HOMO of **5b** originates from the HOMO of **3**, while the HOMOs of **5a** and **6** from the HOMO−1 of **3** (Fig. 9 and S20†). For **5a** and **5b**, the orbital exchanges of the HOMO and HOMO−1 are probably induced by topologies of their π-systems. The planar conformation **5b** stabilizes the HOMO−1 of **3**, while the singly half-twisted conformation **5a** stabilizes the HOMO of **3** because the orbital phase is inverted by the twisted structure. Since the p_z orbital of the central sulfur atom is involved in the HOMO of **5b**, the cyclic 28π-system through the sulfur atom results from the HOMO. In contrast, the HOMOs of **5a** and **6** provide linear π-systems owing to a disruption of the cyclic π-systems at the central sulfur atom. In accordance with the interpretation, the HOMOs of **5c** and **5d** also indicate the cyclic 28π-system and linear π-system, respectively, although we have no experimental evidence of these conformations (Fig. S21†). In addition, the energy gaps between HOMO−1 and HOMO−2 of **5b** and **5c** (*ca.* 0.2 eV) are smaller than those of **5a**, **5d**, and **6**, which also implies an antiaromatic character originating from the macrocyclic π-circuit.[24b] As a result, the HOMO orbital distributions determine whether the hexaphyrins with the β-DTT unit possess a macrocyclic π-circuit or cross-conjugated π-circuit. Therefore, these calculation results imply that the orbital distribution of the HOMO is an important factor to determine the dominant π-circuit for expanded porphyrins. However, it is unclear at this stage why hexaphyrins **5** and **6** prefer a cross-conjugated π-circuit rather than an aromatic π-circuit.

Conclusion

We synthesized and characterized new hexaphyrins **5** and **6** where the dimethine pyrrole unit was replaced with the β-DTT unit. The structure of [28]hexaphyrin **5** was determined to be the twisted Möbius conformation in the single crystal obtained from the CH_2Cl_2 solution. Despite its Möbius topology, the ^{1}H NMR and UV/vis/NIR absorption spectra of **5** in nonpolar solvents (*i.e.*, $CDCl_3$ and CH_2Cl_2) exhibited nonaromatic character, indicating a cross-conjugated π-circuit. In contrast, the ^{1}H NMR and UV/vis/NIR absorption spectra of **5** in polar solvents (*i.e.*, DMF and DMSO) were completely different, which suggests the unexpected unique π-system switching from the cross-conjugated π-circuits in the nonpolar solvent to macrocyclic π-circuits in the polar solvents (and *vice versa*). This π-system switching stems from the change in their molecular topologies with the help of the hydrogen bonds of the NH protons with the polar solvent molecules, which was validated by DFT calculations. More importantly, the DFT calculations provided a theoretical verification of the unprecedented, unique π-system switching of **5** between the Möbius cross-conjugated π-system and the Hückel antiaromatic π-system based on their molecular topologies induced by the solvents (Fig. 10). Although this conclusion was contrary to our initial simple prediction that the switching occurs between the Möbius aromatic π-system and the Hückel cross-conjugated π-system, we successfully corroborated that the β-DTT unit was the effective motif to achieve the π-system switching based on molecular topologies induced by the external stimuli (*i.e.*, solvent). Meanwhile, the ^{1}H NMR and UV/vis/NIR absorption spectra of [26]hexaphyrin **6** exhibited nonaromatic character because of the dominant cross-conjugated π-system despite its planar conformation, which was also supported by DFT calculations. In contrast to **5**, **6** displayed minor solvent effects, suggesting no significant change in its molecular topology. Collectively, hexaphyrins **5** and **6** achieved three-component reversible π-system switching between 28π Möbius cross-conjugated, 28π Hückel macrocyclic, and 26π Hückel cross-

conjugated π-systems by solvent-dependent topological or redox interconversions (Fig. 10). Finally, we explored the origin of the dominant π-circuits of hexaphyrins **5** and **6**. The calculation results suggested that the orbital distribution of the HOMO was the important factor to determine the dominant π-circuit for expanded porphyrins. However, the next challenge is to elucidate the reason why hexaphyrins **5** and **6** prefer a cross-conjugated π-circuit rather than a macrocyclic π-circuit with aromaticity. Furthermore, the insight would provide a hint for novel 26π Möbius antiaromatic systems because **5** prefers a macrocyclic π-circuit despite its antiaromaticity. Overall, this study will open an avenue to create topological molecules of interest by integrating cyclic π-conjugated molecules with the β-DTT unit, where their molecular and π-system topologies are controlled by external stimuli such as solvent as well as conventional protonation and oxidation/reduction.

Conflicts of interest

There are no conflicts to declare.

Acknowledgements

This work was supported by the JSPS (KAKENHI grant numbers JP18K14198 (T. H.) and JP18H03898 (H. I.)).

Notes and references

‡ Crystallographic data for **5**: $C_{56}H_{15}F_{20}N_5S_3\cdot 3.5(CH_2Cl_2)$, $M_r = 1531.15$, triclinic, space group $P\bar{1}$ (no. 2), $a = 13.890(2)$, $b = 14.794(2)$, $c = 16.218(2)$ Å, $\alpha = 96.6694(14)$, $\beta = 96.1744(14)$, $\gamma = 112.8223(16)^\circ$, $V = 3007.7(7)$ Å^3, $\rho_{calcd} = 1.691$ g cm^{-3}, $Z = 2$, 24673 reflections measured, 13239 unique ($R_{int} = 0.0300$), $R_1 = 0.0621$ [$I > 2\sigma(I)$], w$R_2 = 0.1921$ [all data], GOF = 1.096, CCDC 1841655. Crystallographic data for **6**: $2(C_{56}H_{13}F_{20}N_5S_3)\cdot 3$(chlorobenzene), $M_r = 2793.4$, triclinic, space group $P\bar{1}$ (no. 2), $a = 13.765(3)$, $b = 17.271(3)$, $c = 24.190(5)$ Å, $\alpha = 94.738(3)$, $\beta = 102.606(4)$, $\gamma = 93.061(5)^\circ$, $V = 5577.7(19)$ Å^3, $\rho_{calcd} = 1.665$ g cm^{-3}, $Z = 2$, 44377 reflections measured, 23504 unique ($R_{int} = 0.0567$), $R_1 = 0.1121$ [$I > 2\sigma(I)$], w$R_2 = 0.3578$ [all data], GOF = 1.077, CCDC 1841656.

1 H. L. Frisch and E. Wasserman, *J. Am. Chem. Soc.*, 1961, **83**, 3789–3795.

2 (*a*) J. E. Beves, B. A. Blight, C. J. Campbell, D. A. Leigh and R. T. McBurney, *Angew. Chem., Int. Ed.*, 2011, **50**, 9260–9327; (*b*) R. S. Forgan, J.-P. Sauvage and J. F. Stoddart, *Chem. Rev.*, 2011, **111**, 5434–5464; (*c*) J.-F. Ayme, J. E. Beves, C. J. Campbell and D. A. Leigh, *Chem. Soc. Rev.*, 2013, **42**, 1700–1712; (*d*) J.-P. Sauvage, *Angew. Chem., Int. Ed.*, 2017, **56**, 11080–11093.

3 (*a*) Y. Okumura and K. Ito, *Adv. Mater.*, 2001, **13**, 485–487; (*b*) Y. Tezuka and H. Oike, *J. Am. Chem. Soc.*, 2001, **123**, 11570–11576; (*c*) Z. Guan, *Chem.–Asian J.*, 2010, **5**, 1058–1070; (*d*) Y. Tezuka, *Acc. Chem. Res.*, 2017, **50**, 2661–2672; (*e*) E. M. Benetti, M. Divandari, S. N. Ramakrishna, G. Morgese, W. Yan and L. Trachsel, *Chem.–Eur. J.*, 2017, **23**, 12433–12442.

4 E. Heilbronner, *Tetrahedron Lett.*, 1964, **5**, 1923–1928.

5 (*a*) D. Ajami, O. Oeckler, A. Simon and R. Herges, *Nature*, 2003, **426**, 819–821; (*b*) D. Ajami, K. Hess, F. Köhler, C. Näther, O. Oeckler, A. Simon, C. Yamamoto, Y. Okamoto and R. Herges, *Chem.–Eur. J.*, 2006, **12**, 5434–5445.

6 (*a*) Y. Tanaka, S. Saito, S. Mori, N. Aratani, H. Shinokubo, N. Shibata, Y. Higuchi, Z. S. Yoon, K. S. Kim, S. B. Noh, J. K. Park, D. Kim and A. Osuka, *Angew. Chem., Int. Ed.*, 2008, **47**, 681–684; (*b*) J. Sankar, S. Mori, S. Saito, H. Rath, M. Suzuki, Y. Inokuma, H. Shinokubo, K. S. Kim, Z. S. Yoon, J. Shin, J. M. Lim, Y. Matsuzaki, O. Matsushita, A. Muranaka, N. Kobayashi, D. Kim and A. Osuka, *J. Am. Chem. Soc.*, 2008, **130**, 13568–13579; (*c*) S. Tokuji, J.-Y. Shin, K. S. Kim, J. M. Lim, K. Youfu, S. Saito, D. Kim and A. Osuka, *J. Am. Chem. Soc.*, 2009, **131**, 7240–7241; (*d*) M. Inoue, K. S. Kim, M. Suzuki, J. M. Lim, J.-Y. Shin, D. Kim and A. Osuka, *Angew. Chem., Int. Ed.*, 2009, **48**, 6687–6690; (*e*) T. Higashino, M. Inoue and A. Osuka, *J. Org. Chem.*, 2010, **75**, 7958–7961; (*f*) M. Inoue and A. Osuka, *Angew. Chem., Int. Ed.*, 2010, **49**, 9488–9491; (*g*) M. Inoue, T. Yoneda, K. Youfu, N. Aratani and A. Osuka, *Chem.–Eur. J.*, 2011, **17**, 9028–9031; (*h*) S. Ishida, T. Tanaka, J. M. Lim, D. Kim and A. Osuka, *Chem.–Eur. J.*, 2014, **20**, 8274–8278; (*i*) T. Higashino, T. Soya, W. Kim, D. Kim and A. Osuka, *Angew. Chem., Int. Ed.*, 2015, **54**, 5456–5459; (*j*) H. Ruffin, G. N. M. Boussambe, T. Roisnel, V. Dorcet, B. Boitrel and S. Le Gac, *J. Am. Chem. Soc.*, 2017, **139**, 13847–13857; (*k*) M. Izawa, T. Kim, S. Ishida, T. Tanaka, T. Mori, D. Kim and A. Osuka, *Angew. Chem., Int. Ed.*, 2017, **56**, 3982–3986.

7 (*a*) M. Stepień, L. Latos-Grażyński, N. Sprutta, P. Chwalisz and L. Szterenberg, *Angew. Chem., Int. Ed.*, 2007, **46**, 7869–7873; (*b*) S. Saito, J.-Y. Shin, J. M. Lim, K. S. Kim, D. Kim and A. Osuka, *Angew. Chem., Int. Ed.*, 2008, **47**, 9657–9660; (*c*) J. K. Park, Z. S. Yoon, M. Yoon, K. S. Kim, S. Mori, J. Shin, A. Osuka and D. Kim, *J. Am. Chem. Soc.*, 2008, **130**, 1824–1825; (*d*) J. M. Lim, J.-Y. Shin, Y. Tanaka, S. Saito, A. Osuka and D. Kim, *J. Am. Chem. Soc.*, 2010, **132**, 3105–3114; (*e*) S. Gokulnath, M. Toganoh, K. Yamaguchi, S. Mori, H. Uno and H. Furuta, *Dalton Trans.*, 2012, **41**, 6283–6290; (*f*) T. Yoneda, Y. M. Sung, J. M. Lim, D. Kim and A. Osuka, *Angew. Chem., Int. Ed.*, 2014, **53**, 13169–13173; (*g*) B. Szyszko, N. Sprutta, P. Chwalisz, M. Stępień and L. Latos-Grażyński, *Chem.–Eur. J.*, 2014, **20**, 1985–1997; (*h*) A. Ghosh, A. Chaudhary, A. Srinivasan, C. H. Suresh and T. K. Chandrashekar, *Chem.–Eur. J.*, 2016, **22**, 3942–3946; (*i*) A. Mallick, J. Oh, M. A. Majewski, M. Stępień, D. Kim and H. Rath, *J. Org. Chem.*, 2017, **82**, 556–566.

8 (*a*) E. Pacholska-Dudziak, J. Skonieczny, M. Pawlicki, L. Szterenberg, Z. Ciunik and L. Latos-Grazyński, *J. Am. Chem. Soc.*, 2008, **130**, 6182–6195; (*b*) T. Higashino, J. M. Lim, T. Miura, S. Saito, J.-Y. Shin, D. Kim and A. Osuka, *Angew. Chem., Int. Ed.*, 2010, **49**, 4950–4954; (*c*) T. Higashino, B. S. Lee, J. M. Lim, D. Kim and A. Osuka, *Angew. Chem., Int. Ed.*, 2012, **51**, 13105–13108.

9 (*a*) T. D. Lash, *Angew. Chem., Int. Ed.*, 2000, **39**, 1763–1767; (*b*) J. L. Sessler and D. Seidel, *Angew. Chem., Int. Ed.*, 2003, **42**, 5134–5175; (*c*) S. Saito and A. Osuka, *Angew. Chem., Int. Ed.*, 2011, **50**, 4342–4373; (*d*) M. Stępień, N. Sprutta and L. Latos-Grażyński, *Angew. Chem., Int. Ed.*, 2011, **50**, 4288–4340; (*e*) T. Tanaka and A. Osuka, *Chem. Rev.*, 2017, **117**,

2584–2640; (*f*) B. Szyszko, M. J. Białek, E. Pacholska-Dudziak and L. Latos-Grażyński, *Chem. Rev.*, 2017, **117**, 2839–2909.

10 (*a*) E. Marcos, J. M. Anglada and M. Torrent-Sucarrat, *J. Phys. Chem. C*, 2012, **116**, 24358–24366; (*b*) M. Alonso, P. Geerlings and F. de Proft, *Chem.–Eur. J.*, 2012, **18**, 10916–10928; (*c*) E. Marcos, J. M. Anglada and M. Torrent-Sucarrat, *J. Org. Chem.*, 2014, **79**, 5036–5046; (*d*) M. Alonso, B. Pinter, P. Geerlings and F. De Proft, *Chem.–Eur. J.*, 2015, **21**, 17631–17638.

11 (*a*) A. Osuka and S. Saito, *Chem. Commun.*, 2011, **47**, 4330–4339; (*b*) M. Pawlicki and L. Latos-Grażyński, *Chem.–Asian J.*, 2015, **10**, 1438–1451; (*c*) Y. M. Sung, J. Oh, W.-Y. Cha, W. Kim, J. M. Lim, M.-C. Yoon and D. Kim, *Chem. Rev.*, 2017, **117**, 2257–2312; (*d*) M. Torrent-Sucarrat, S. Navarro, E. Marcos, J. M. Anglada and J. M. Luis, *J. Phys. Chem. C*, 2017, **121**, 19348–19357; (*e*) T. Stuyver, M. Perrin, P. Geerlings, F. De Proft and M. Alonso, *J. Am. Chem. Soc.*, 2018, **140**, 1313–1326.

12 (*a*) T. Koide, K. Youfu, S. Saito and A. Osuka, *Chem. Commun.*, 2009, 6047–6049; (*b*) J.-Y. Shin, J. M. Lim, Z. S. Yoon, K. S. Kim, M.-C. Yoon, S. Hiroto, H. Shinokubo, S. Shimizu, A. Osuka and D. Kim, *J. Phys. Chem. B*, 2009, **113**, 5794–5802; (*c*) M. Stępień, B. Szyszko and L. Latos-Grażyński, *J. Am. Chem. Soc.*, 2010, **132**, 3140–3152; (*d*) S. Ishida, T. Higashino, S. Mori, H. Mori, N. Aratani, T. Tanaka, J. M. Lim, D. Kim and A. Osuka, *Angew. Chem., Int. Ed.*, 2014, **53**, 3427–3431; (*e*) K. Naoda, H. Mori, J. Oh, K. H. Park, D. Kim and A. Osuka, *J. Org. Chem.*, 2015, **80**, 11726–11733; (*f*) T. Soya, H. Mori, Y. Hong, Y. H. Koo, D. Kim and A. Osuka, *Angew. Chem., Int. Ed.*, 2017, **56**, 3232–3236.

13 (*a*) M.-C. Yoon, J.-Y. Shin, J. M. Lim, S. Saito, T. Yoneda, A. Osuka and D. Kim, *Chem.–Eur. J.*, 2011, **17**, 6707–6715; (*b*) T. Higashino and A. Osuka, *Chem. Sci.*, 2013, **4**, 1087–1091.

14 T. Higashino, A. Kumagai and H. Imahori, *Chem. Commun.*, 2017, **53**, 5091–5094.

15 (*a*) M. Toganoh and H. Furuta, *Chem. Commun.*, 2012, **48**, 937–954; (*b*) H. Furuta, T. Ishizuka, A. Osuka, H. Dejima, H. Nakagawa and Y. Ishikawa, *J. Am. Chem. Soc.*, 2001, **123**, 6207–6208; (*c*) M. Toganoh, T. Yamamoto, T. Hihara, H. Akimaru and H. Furuta, *Org. Biomol. Chem.*, 2012, **10**, 4367–4374; (*d*) C. J. Ziegler, N. R. Erickson, M. R. Dalby and V. N. Nemykin, *J. Phys. Chem. A*, 2013, **117**, 11499–11508; (*e*) R. Sakashita, Y. Oka, H. Akimaru, P. E. Kesavan, M. Ishida, M. Toganoh, T. Ishizuka, S. Mori and H. Furuta, *J. Org. Chem.*, 2017, **82**, 8686–8696.

16 (*a*) T. K. Chandrashekar and S. Venkatraman, *Acc. Chem. Res.*, 2003, **36**, 676–691; (*b*) N. Shivran, S. C. Gadekar and V. G. Anand, *Chem.–Asian J.*, 2017, **12**, 6–20; (*c*) T. Chatterjee, A. Srinivasan, M. Ravikanth and T. K. Chandrashekar, *Chem. Rev.*, 2017, **117**, 3329–3376.

17 V. G. Anand, S. Saito, S. Shimizu and A. Osuka, *Angew. Chem., Int. Ed.*, 2005, **44**, 7244–7248.

18 Quite recently, Osuka and co-workers reported decaphyrin with the contribution of the Möbius aromatic thia[28] hexaphyrin segment. See ref 11*e*.

19 B. Koszarna and D. T. Gryko, *J. Org. Chem.*, 2006, **71**, 3707–3717.

20 K. Naoda, Y. M. Sung, J. M. Lim, D. Kim and A. Osuka, *Chem.–Eur. J.*, 2014, **20**, 7698–7705.

21 (*a*) L. K. Frensch, K. Pröpper, M. John, S. Demeshko, C. Brückner and F. Meyer, *Angew. Chem., Int. Ed.*, 2011, **50**, 1420–1424; (*b*) E. Ganapathi, W.-Z. Lee and M. Ravikanth, *J. Org. Chem.*, 2014, **79**, 9603–9612; (*c*) Z. Zhou, Y. Chang, S. Shimizu, J. Mack, C. Schütt, R. Herges, Z. Shen and N. Kobayashi, *Angew. Chem., Int. Ed.*, 2014, **53**, 6563–6567.

22 (*a*) A. J. Pistner, G. P. A. Yap and J. Rosenthal, *J. Phys. Chem. C*, 2012, **116**, 16918–16924; (*b*) A. J. Pistner, D. A. Lutterman, M. J. Ghidiu, E. Walker, G. P. A. Yap and J. Rosenthal, *J. Phys. Chem. C*, 2014, **118**, 14124–14132; (*c*) A. M. Bruce, E. S. Weyburne, J. T. Engle, C. J. Ziegler and G. R. Geier, *J. Org. Chem.*, 2014, **79**, 5664–5672; (*d*) A. S. Aslam, J.-H. Hong, J.-H. Shin and D.-G. Cho, *Angew. Chem., Int. Ed.*, 2017, **56**, 16247–16251; (*e*) T. Higashino and A. Osuka, *Chem.–Asian J.*, 2013, **8**, 1994–2002; (*f*) J. Kong, J. Shao, C. Li, D. Qi, M. Li, X. Liang, W. Zhu, J. Jiang and Y. Xie, *Org. Lett.*, 2017, **19**, 650–653.

23 J.-Y. Shin, K. S. Kim, M.-C. Yoon, J. M. Lim, Z. S. Yoon, A. Osuka and D. Kim, *Chem. Soc. Rev.*, 2010, **39**, 2751–2767.

24 (*a*) W.-Y. Cha, T. Soya, T. Tanaka, H. Mori, Y. Hong, S. Lee, K. H. Park, A. Osuka and D. Kim, *Chem. Commun.*, 2016, **52**, 6076–6078; (*b*) T. Woller, P. Geerlings, F. De Proft, B. Champagne and M. Alonso, *Molecules*, 2018, **23**, 1333.

25 M. Torrent-Sucarrat, S. Navarro, F. P. Cossío, J. M. Anglada and J. M. Luis, *J. Comput. Chem.*, 2017, **38**, 2819–2828.

26 I. Casademont-Reig, T. Woller, J. Contreras-García, M. Alonso, M. Torrent-Sucarrat and E. Matito, *Phys. Chem. Chem. Phys.*, 2018, **20**, 2787–2796.

27 (*a*) P. v. R. Schleyer, C. Maerker, A. Dransfeld, H. Jiao and N. J. R. v. E. Hommes, *J. Am. Chem. Soc.*, 1996, **118**, 6317–6318; (*b*) Z. Chen, C. S. Wannere, C. Corminboeuf, R. Puchta and P. v. R. Schleyer, *Chem. Rev.*, 2005, **105**, 3842–3888.

28 (*a*) S. Mori and A. Osuka, *J. Am. Chem. Soc.*, 2005, **127**, 8030–8031; (*b*) H. Rath, N. Aratani, J. M. Lim, J. S. Lee, D. Kim, H. Shinokubo and A. Osuka, *Chem. Commun.*, 2009, 3762–3764; (*c*) T. Yoneda, T. Kim, T. Soya, S. Neya, J. Oh, D. Kim and A. Osuka, *Chem.–Eur. J.*, 2016, **22**, 4413–4417.

29 T. M. Krygowski and M. K. Cyrański, *Chem. Rev.*, 2001, **101**, 1385–1420.

30 K. Naoda and A. Osuka, *Chem.–Asian J.*, 2016, **11**, 2849–2853.

31 Although bond lengths and bond orders are not sufficient to understand the dominant π-circuits of our compounds, recently proposed electronic indices[26] and special ring current density[32] could provide understanding of conjugation pathways in expanded porphyrins. However, at this stage these calculations cannot be performed on commercial programs such as Gaussian[33] that we can use currently. The special ring current density calculation could be used to distinguish from cross-conjugated to macrocyclic networks because the antiaromatic character can be evaluated by magnetically induced currents. Such

challenging calculations will be done separately and reported elsewhere in the future.

32 H. Fliegl, D. Sundholm, S. Taubert and F. Pichierri, *J. Phys. Chem. A*, 2010, **114**, 7153–7161.

33 M. J. Frisch, G. W. Trucks, H. B. Schlegel, G. E. Scuseria, M. A. Robb, J. R. Cheeseman, G. Scalmani, V. Barone, B. Mennucci, G. A. Petersson, H. Nakatsuji, M. Caricato, X. Li, H. P. Hratchian, A. F. Izmaylov, J. Bloino, G. Zheng, J. L. Sonnenberg, M. Hada, M. Ehara, K. Toyota, R. Fukuda, J. Hasegawa, M. Ishida, T. Nakajima, Y. Honda, O. Kitao, H. Nakai, T. Vreven, J. A. Montgomery, Jr., J. E. Peralta, F. Ogliaro, M. Bearpark, J. J. Heyd, E. Brothers, K. N. Kudin, V. N. Staroverov, T. Keith, R. Kobayashi, J. Normand, K. Raghavachari, A. Rendell, J. C. Burant, S. S. Iyengar, J. Tomasi, M. Cossi, N. Rega, J. M. Millam, M. Klene, J. E. Knox, J. B. Cross, V. Bakken, C. Adamo, J. Jaramillo, R. Gomperts, R. E. Stratmann, O. Yazyev, A. J. Austin, R. Cammi, C. Pomelli, J. W. Ochterski, R. L. Martin, K. Morokuma, V. G. Zakrzewski, G. A. Voth, P. Salvador, J. J. Dannenberg, S. Dapprich, A. D. Daniels, O. Farkas, J. B. Foresman, J. V. Ortiz, J. Cioslowski and D. J. Fox, *Gaussian 09, revision D.01*, Gaussian, Inc., Wallingford, CT, 2013.